

## **SURFACE ROUGHNESS EVALUATION OF CYLINDRICAL MACHINED SURFACES**

*B.Dhanasekar<sup>1</sup>, B.Ramamoorthy<sup>2</sup>*

<sup>1</sup> Research scholar, Department of Mechanical Engineering, IITMadras, Chennai 60036, India, sekar@iitm.ac.in

<sup>2</sup> Professor, Department of Mechanical Engineering, IITMadras, Chennai 60036, India, ramoo@iitm.ac.in

**Abstract:** Computer vision based on digital image processing is a fast emerging as a research tool in various branches of engineering. In manufacturing engineering environment it is mainly used for robot applications like inspection, recognition and navigation. In this work the area of application is extended to incorporate its use in metrological applications where the objective of the work had been to evaluate the surface roughness of cylindrical machined surface (turned) using machine vision technique. Basically to estimate the roughness of a cylindrical surface based on the images would pose a fundamental problem as the surface being a doubly curved one. This image distortion need to be resolved before proceeding to the evaluation of roughness of such surfaces. This study uses involved the geometric correction technique by developing an algorithm in which distortion encountered in the projection of cylindrical machined surface image is rectified. The quantification for surface roughness after opening the surfaces is performed using the surface image parameters (spatial frequency (F), arithmetic mean value ( $G_a$ ) and standard deviation (STD)). Then the Group Method of Data Handling (GMDH) technique was used to obtain an analytical relationship of the roughness parameters calculated using the digital surface image and the stylus instrument values. An analysis based on the comparison to make sure that the present approach of estimation of surface finish based on the digital processed image could be implemented in practice, is presented in this paper..

**Keywords:** Machine vision, Turning, Surface roughness, GMDH

### **1. INTRODUCTION**

With growing demand of industrial automation in manufacturing, machine vision plays an important role in quality inspection and process monitoring. Surface roughness inspection is one of the essential quality control processes that is carried out to ensure that manufactured parts conform to specified standards. This kind of inspection is normally done through the use of stylus type instruments, which correlate the motion of a diamond-tipped stylus to the roughness of the surface under investigation. The major disadvantage of using a stylus instrument for such measurements is that it requires direct physical contact,

which limits the measuring speed. In addition, the instrument readings are based on a limited number of line samplings, which may not represent the real characteristics of the surface. This kind of deviation may cause serious errors in the surface quality assessment especially when the surface profile is periodic. Because of these drawbacks, contact type instruments are not suitable for high-speed automated inspection. Previous researchers using machine vision techniques for surface texture assessment have covered several calculated parameters, with stylus profilometer measurements of average roughness (area) performed on the same surface. Luk et al.[1] utilized statistical parameters, derived from the grey level intensity histogram such as the range and the mean value of the distribution and correlated them with the  $R_a$  value determined from the stylus method. Al-Kindi et al.[2] implemented a technique utilizing a roughness parameter based on both the spacing between grey level peaks and the number of grey level peaks per unit length of a scanned line in the grey level image to estimate the surface roughness. Du-Ming Tsai et al.[3] employed a two-dimensional Fourier transform of a cast surface in both the grey level image and binary image to estimate the surface roughness of castings (for surfaces with  $R_a > 10\mu\text{m}$ ). Pre-processing for eliminating effects due to illumination problems and noise was reported by Ramamoorthy et al. [4]. Younis [5] has analysed the pattern of scattered light from a surface to derive an optical roughness parameter for different materials. The comparison of the optical roughness parameter and the average roughness obtained using a stylus instrument for different materials was found to be correlating well and highly consistent.

Lee et al. [6] have used a self-organizing adaptive learning tool called polynomial network to estimate the surface roughness of turned components manufactured using conventional processes. But in their study, curvature effect on surface image is not taken into consideration. Ramamoorthy et al. [7] estimated optical roughness value ( $G_a$ ) based on the digital images initially magnified using cubic convolution technique and then processed further using Linear Edge Crispening algorithm. It was reported that the  $G_a$  values correlated well with the stylus instrument surface roughness ( $R_a$ ) values measured for the components

manufactured using the machining process such as shaping, milling and grinding.

In this paper, the cylindrical machined surfaces (turning) are first opened by using an algorithm as shown in Fig. [1]. The surfaces are opened before analysis there by suitable comparisons can be obtained with stylus value ( $R_a$ ). After opening the images of machined surfaces, the roughness parameters of image textures (spatial frequency, arithmetic mean value and standard deviation) are evaluated. Then GMDH network is used to predict the surface roughness values using these parameters as input values. The predicted surface roughness values are compared with the stylus roughness values and analysed in this paper.

## 2. EXPERIMENTAL PROCEDURE

The experiments were carried out by manufacturing cylindrical specimens (turned) based on L27 orthogonal array as shown in Table 1. Surfaces with different textures are obtained by controlling the machining parameters of these processes. The machining parameters were selected by varying the cutting speed in the range 250–710 m min<sup>-1</sup>, the feed rate in the range 0.1–0.18 mm rev<sup>-1</sup>, the depth of cut in the range 0.5–1.5 mm, and the average surface roughness  $R_a$  in the range 0.3–4 μm. The images of the specimens are grabbed with a Matrox vision system (CCD camera: Pulnix - TM6, 768x565 pixels, with Image processing hardware with 4 frame buffers and 1/30 s frame speed). The average roughness values ( $R_a$ ) of the specimens are obtained with a stylus instrument with 4.8mm as sampling length and 0.8 mm cut off length as per international standards. For the analysis of surface image, the pixel matrix is restricted to the size of 100x150 pixels to enable reduction in computer memory and processing speed. The input image is quantized to a eight-bit gray level.

## 3. IMAGE PROCESSING FOR OPENING CYLINDRICAL SURFACE

The captured images are preprocessed before surface roughness feature extraction. The cylindrical surfaces are first opened before analysis by using the principles of cartography. The science of cartography [8] is concerned with producing two dimensional maps from solids of revolution like sphere, cones or cylinders. This is a complicated problem as the surfaces cannot be easily flattened without distortion. This problem is usually solved by the projection of solids of revolution like spheres on to cylinders or cones followed by unrolling of these surfaces. The problem of distortion has to be avoided by removing the holing effect caused due to the unrolling of these surfaces.

For cylindrical surfaces under consideration the map properties are satisfied by grabbing the images so that the entire cylinder is visible. This ensures that the distortion effects are removed as the distance between the object and the camera is large compared to the object size. The surface on which surface features can be projected to form a two dimensional map is a plane from a cylinder. The cylinder is cut along a line parallel to the axis and unrolled to form a

map. This technique is used only for the location of points of interest on the opened image and the gray values at these positions should also be considered as they affect the textures of the opened images. These distortions are to be studied as they play an important role in the textures and also as the properties get greatly modified by a change in the gray values of the pixels of these images. Hence these factors are studied by first developing an algorithm for the unrolling of cylinders.

Basic steps involved in the algorithm

1. Determine the output image requirements.
2. Digitise the input image into pixels.
3. Determine the relation between the output image and input image pixels.
4. Formulate the equation required for the pixel interpolation.
5. Based on the equation deduce the input pixel positions in the output image.
6. Fill the corresponding output image pixels with the same gray values as the input image pixels.
7. Remove holes to fill the incomplete pixels by averaging the immediate neighbours (Bicubic interpolation).
8. Repeat for all scan lines
9. Redisplay the output pixel array as image.

The sample images of the turned specimen before and after opened images are shown in Fig.2.

## 4. EXTRACTION OF SURFACE ROUGHNESS FEATURES

In this study, after opening the images of machined (turned) surfaces, the roughness parameters of image textures (spatial frequency, arithmetic mean value and standard deviation) are extracted. The surface roughness parameter used throughout in this study is the average surface roughness ( $R_a$ ) as it is the most widely used and accepted surface finish parameter by researchers and in industry as well. It is the arithmetic average of the absolute value of the heights of roughness irregularities from the mean value measured within a sampling length of 8 mm [9] that is

$$R_a = \frac{\left( \sum_{i=1}^n |y_i| \right)}{n} \quad (1)$$

where  $y_i$  is the height of roughness irregularities from the mean value and  $n$  is the number of sampling data. In this study, a feature of the surface image, called the arithmetic average of the grey level, is used to predict the actual surface roughness of the work piece. The arithmetic average of the grey level  $G_a$  can be expressed as

$$G_a = \sqrt{\sum (F_{m,n} - F_{i,j})^2 / (8F_{av})} \quad (2)$$

Where:  $(m,n) = (i, j-1), (i,j+1), (i+1,j), (i+1,j-1)$

$(i+1,j+1), (i-1,j), (i-1,j-1)$  and  $(i-1,j+1)$

$$F_{av} = \sum F_{m,n} / 8$$

The fluctuation is the natural property of surface roughness consisting of high, medium and low frequency variations. The standard deviation represents the overall variation with respect to the mean.

## 5. GMDH FOR SURFACE ROUGHNESS ASSESSMENT

In this paper, Group method of data handling (GMDH) is used to predict the surface roughness parameter  $R_v$  using parameters calculated from the images namely spatial frequency, arithmetic mean value and standard deviation. Then, this predicted/estimated value is compared with that of the surface roughness obtained using a stylus instrument ( $R_a$ ) for machined surfaces after opening of cylindrical (turned) surface and are presented in Tables 1 and 2. The GMDH is an established technique for obtaining the polynomial description of a stochastic system from a small amount of experimental data. The GMDH procedure [10] uses partial description in the form of second order polynomials with

$$y_k = b_0 + b_1X_i + b_2X_j + b_3X_i^2 + b_4X_j^2 + b_5X_iX_j \quad (3)$$

Where  $Y_k$  denotes an intermediate variable and  $X_i, X_j$  are a pair-wise combination of normalized input variables and  $b_0, b_1, \dots, b_5$  are the coefficients. The accuracy of the GMDH is often extremely better than the ordinary regression methods due to the reason that the minimum mean square error yields optimum value only in the small domain where the number of the regression polynomial members (regression coefficients) are much less than the number of points of interpolation (experimental data points or observations) Ivakhnenko [11]. GMDH equations used for prediction of surface roughness are listed in the appendix.

## 6. EXPERIMENTAL VERIFICATION AND DISCUSSIONS

To evaluate the developed network for measuring the surface roughness of turned workpieces, 8 more turned specimens using different cutting parameters were manufactured (Table 2). The GMDH model was evaluated in terms of the RMSE and the  $R^2$  value for the experimental and testing data and are shown in Table 1 and 2. The RMSE is used to determine the prediction performance and the coefficient of determination ( $R^2$ ) was used to identify the closeness of fit. In the polynomial network, the regression coefficients of the polynomial at each stage are calculated as shown in appendix by employing the least square approximation technique. The predicted surface roughness ( $R_v$ ) obtained by using the polynomial network at each stage is compared with the experimental data ( $R_a$ ) and the RMSE at each layer. It was observed that the RMSE reduced considerably within the initial few layers as shown in Fig.[3] and in order to reduce the computational effort, three hidden layers are considered. A comparison of  $R_v$  (measured by the vision system) and  $R_a$  (measured by the stylus method) are shown in Fig. 4 and 5. The maximum error for training is 5.2% and for testing is 7.2%.

## 7. CONCLUSIONS

This paper has explained the use of computer vision techniques to inspect the surface roughness of components generated using cylindrical (turned) components which involves the geometric correction technique by the development of an algorithm in which distortion problem encountered in the projection of cylindrical machined is rectified. The GMDH network was used to predict the surface roughness values using the input parameters (spatial frequency, arithmetic mean value and standard deviation) calculated based on images. It was observed that the calculated/predicted surface parameters based on the digital images after opening of cylindrical (turned) surface had a better correlation (i.e. higher correlation coefficient) with the average stylus surface roughness parameter measured for the manufactured components. Therefore, this concept/approach could be extended for estimation of roughness of other surfaces manufactured by processes such as cylindrical grinding.

## REFERENCES

- [1] F. Luk, V. Hyunh and W. North, "Measurement of surface roughness by a machine vision system," *Journal of Physics E Scientific Instruments* Vol. 22, pp. 977-980, 1989.
- [2] G. A. Al-kind, R. M. Baul and K. F. Gill, "An application of machine vision in the automated inspection of engineering surfaces," *International journal of Production Research* Vol. 2, pp. 241-253, 1992
- [3] Du-Ming Tsai and Chi-Fong Tseng, "Surface roughness classification for castings," *Pattern Recognition, Journal of Physics E Scientific Instruments* Vol. 32, pp. 389-405, 1999.
- [4] M.Kiran, B.Ramamoorthy and V.Radhakrishnan, "Measurement of surface roughness by a machine vision system," *Journal of Physics E Scientific Instruments* Vol. 22, pp. 977-980, 1989
- [5] Younis MA, "On line surface roughness measurements using image processing towards an adaptive control," *Computers industry Engineering* Vol. 35, pp. 49-52, 1998
- [6] Lee BY, Tarng YS, "Surface roughness inspection by computer vision in turning operations," *International journal for Machine tools and Manufacture* Vol. 41, pp. 1251-1263, 2001.
- [7] Rajneesh kumar, Dhanasekar B, Ramamoorthy B, "Application of digital image magnification for surface roughness evaluation using machine vision," *International journal for Machine tools and Manufacture* Vol. 45, pp. 228-234, 2005.
- [8] Castleman KR, "Digital image processing", Prentice Hall Englewood cliffs, New Jersey, 1979.

[9] ISO 4288:1996, Geometrical product specification (GPS)-surface texture:profile method-Terms definitions and surface texture parameters, Int. Std. Org, Geneva.

[10] Farlow SJ, "The GMDH algorithm, self-organizing methods in modeling," GMDH type algorithms, 1984

[11] Ivakhenko AG, "Polynomial theory of complex systems," IEEE Trans Syst Man Cyb 1(4), 364-378, 1971

**APPENDIX**

*GMDH model for surface roughness evaluation*

The partial descriptions for each layer are as follows:

In the **Third** layer

$$R_a = 1.1170 - 3.3311 U_1 + 3.3311 U_2 - 5.6659 U_1^2 - 7.0052 U_2^2 + 12.8294 U_1 U_2$$

In the **Second** layer

$$U_1 = 9.9467 + 13.4792 Y_1 - 19.3592 Y_2 - 1.0204 Y_1^2 + 4.7157 Y_2^2 - 2.4986 Y_1 Y_2$$

$$U_2 = -9.3941 + 5.9196 Y_1 + 2.1140 Y_3 - 0.4695 Y_1^2 + 0.0750 Y_3^2 - 0.9057 Y_1 Y_3$$

In the **First** layer

$$Y_1 = 0.0070 - 0.0009 F - 0.0206 Ga - 1.0124 Ga^2 + 0.0196 F.Ga$$

$$Y_2 = 0.0009 - 0.0010 F + 0.0007 STD + 0.0001 F.STD$$

$$Y_3 = -0.0031 + 0.1169 Ga + 0.003 STD - 0.7337 Ga^2 - 0.0016 Ga.STD$$

**FIGURES AND TABLES**

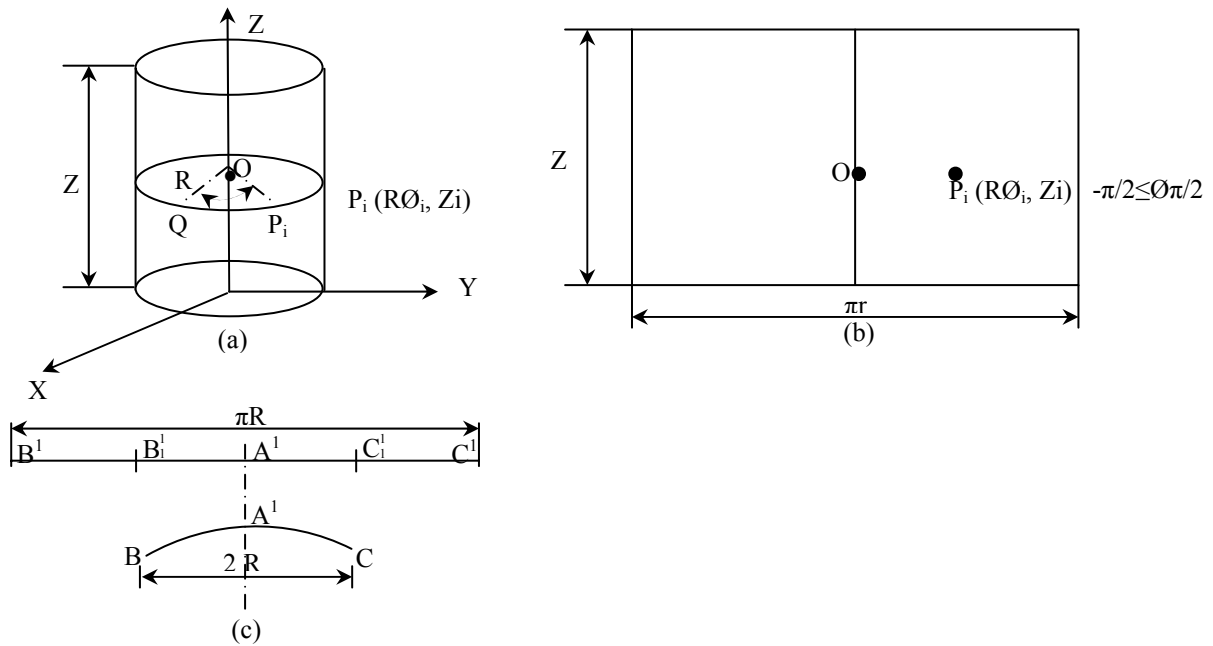


**Fig.1.** (a) Cylindrical surface with point P<sub>i</sub> on the surface before opening  
 (b) Point P on the one half opened surface of the cylindrical surface  
 (c) Semicircle and equivalent length

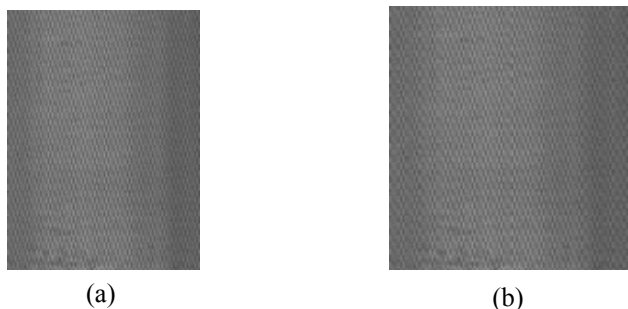


**Fig.2.** (a) Turned cylindrical specimen  
 (b) Flattened image of turned specimen using the algorithm

**Table 1.** Experimental texture of turned workpiece surface and surface roughness for training database.

| Data No | Roughness features of image texture |                |              |                   |                          |          |
|---------|-------------------------------------|----------------|--------------|-------------------|--------------------------|----------|
|         | F                                   | G <sub>a</sub> | STD          | R <sub>v</sub>    | Stylus (R <sub>a</sub> ) | Error    |
|         | (line/mm)                           | (gray level)   | (gray level) | ( $\mu\text{m}$ ) | ( $\mu\text{m}$ )        | %        |
| 1       | 10                                  | 0.0511         | 14.2107      | 2.0676            | 2.071                    | 0.164172 |
| 2       | 10                                  | 0.0503         | 15.9108      | 2.1728            | 2.1961                   | 1.060972 |
| 3       | 10                                  | 0.0655         | 18.4926      | 2.9679            | 2.8612                   | 3.729205 |
| 4       | 7.142857                            | 0.0486         | 14.1948      | 2.9738            | 2.851                    | 4.307261 |
| 5       | 7.142857                            | 0.0561         | 17.0567      | 2.9932            | 2.9035                   | 3.089375 |
| 6       | 7.142857                            | 0.063          | 17.7414      | 2.9906            | 2.987                    | 0.120522 |
| 7       | 5.555556                            | 0.0711         | 19.0779      | 2.5314            | 2.47                     | 2.48583  |
| 8       | 5.555556                            | 0.0593         | 15.6272      | 3.0183            | 2.904                    | 3.93595  |
| 9       | 5.555556                            | 0.0645         | 17.8781      | 2.9394            | 3.066                    | 4.129159 |
| 10      | 10                                  | 0.0501         | 14.8349      | 2.0996            | 2.09                     | 0.45933  |
| 11      | 10                                  | 0.059          | 16.2524      | 2.9393            | 2.848                    | 3.205758 |
| 12      | 10                                  | 0.0594         | 16.7555      | 2.9538            | 2.934                    | 0.674847 |
| 13      | 7.142857                            | 0.0481         | 15.5011      | 2.9471            | 3.004                    | 1.894141 |
| 14      | 7.142857                            | 0.0471         | 14.5537      | 2.9724            | 3.007                    | 1.150648 |
| 15      | 7.142857                            | 0.0473         | 14.9646      | 2.958             | 3.086                    | 4.147764 |
| 16      | 5.555556                            | 0.0581         | 16.7164      | 3.0004            | 3.015                    | 0.484245 |
| 17      | 5.555556                            | 0.0596         | 16.6379      | 3.0156            | 3.007                    | 0.285999 |
| 18      | 5.555556                            | 0.0564         | 15.8304      | 2.9873            | 3.104                    | 3.759665 |
| 19      | 10                                  | 0.0569         | 15.7176      | 2.803             | 2.851                    | 1.68362  |
| 20      | 10                                  | 0.06           | 16.1454      | 2.9812            | 2.971                    | 0.343319 |
| 21      | 10                                  | 0.0642         | 17.0673      | 2.9831            | 3.0768                   | 3.045372 |
| 22      | 7.142857                            | 0.0559         | 15.2274      | 2.9824            | 2.835                    | 5.199295 |
| 23      | 7.142857                            | 0.0591         | 15.0064      | 3.0011            | 2.958                    | 1.457066 |
| 24      | 7.142857                            | 0.057          | 16.2987      | 3.0025            | 3.131                    | 4.10412  |
| 25      | 5.555556                            | 0.061          | 17.9483      | 2.9786            | 3.009                    | 1.010302 |
| 26      | 5.555556                            | 0.0478         | 13.3234      | 3.1585            | 3.159                    | 0.015828 |
| 27      | 5.555556                            | 0.0604         | 16.2159      | 3.0217            | 3.045                    | 0.765189 |

**Table 2.** Experimental texture of turned workpiece surface and surface roughness for testing database

| Data No | Roughness features of image texture |                |              |                   |                          |             |
|---------|-------------------------------------|----------------|--------------|-------------------|--------------------------|-------------|
|         | F                                   | G <sub>a</sub> | STD          | R <sub>v</sub>    | Stylus (R <sub>a</sub> ) | Error       |
|         | (line/mm)                           | (gray level)   | (gray level) | ( $\mu\text{m}$ ) | ( $\mu\text{m}$ )        | %           |
| 1       | 6.25                                | 0.0567         | 17.299       | 2.9753            | 2.901                    | 2.561185798 |
| 2       | 8                                   | 0.0579         | 17.2995      | 2.9999            | 3.09                     | 2.915857605 |
| 3       | 8.928571                            | 0.0493         | 15.8681      | 2.4919            | 2.52                     | 1.115079365 |
| 4       | 7.142857                            | 0.0575         | 16.4378      | 3.0053            | 2.991                    | 0.47810097  |
| 5       | 5.555556                            | 0.0572         | 16.4814      | 2.9924            | 3.212                    | 6.836861768 |
| 6       | 8.928571                            | 0.055          | 16.022       | 2.8977            | 3.001                    | 3.442185938 |
| 7       | 8                                   | 0.0549         | 16.2493      | 2.9714            | 3.201                    | 7.172758513 |
| 8       | 6.25                                | 0.0476         | 14.5586      | 3.0876            | 3.231                    | 4.43825441  |

Note: F: Spatial frequency Ga: Airthmetic gray value STD: Standard deviation R<sub>v</sub>:Vision roughness

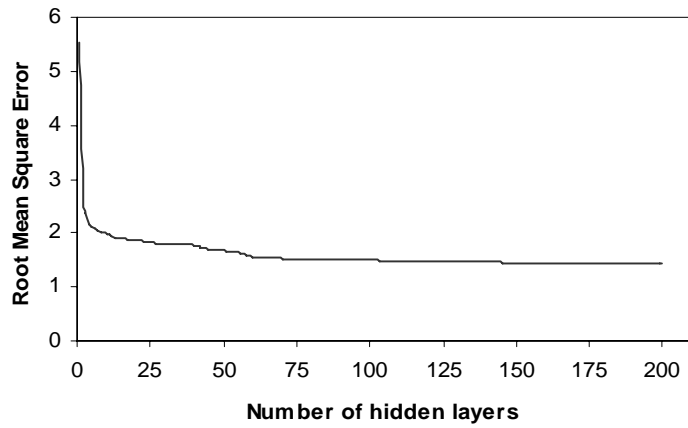


**Fig. 3.** The convergence pattern obtained with GMDH model with number of hidden layers

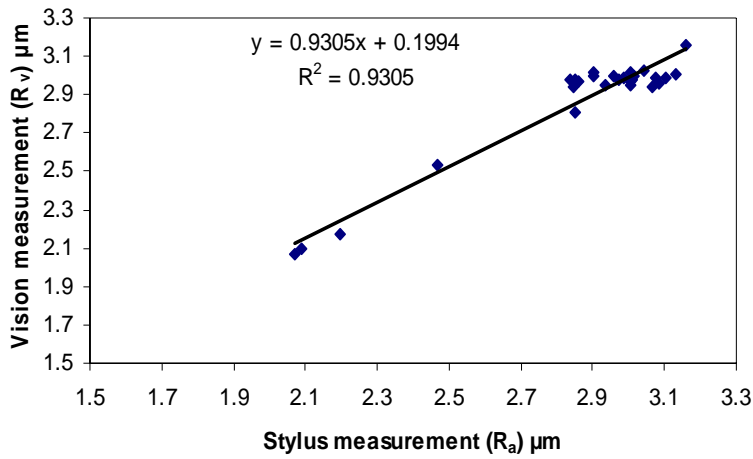


**Fig. 4.** Correlation of estimated roughness values using Vision approach and Stylus approach for training database

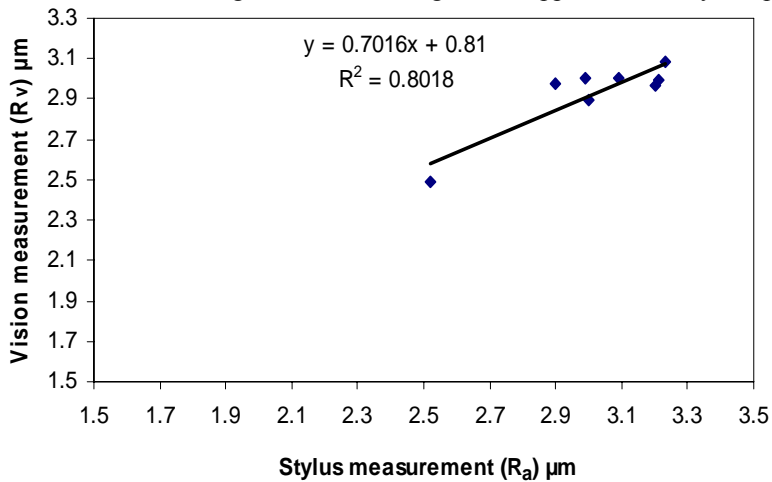


**Fig. 5.** Correlation of estimated roughness values using Vision approach and Stylus approach for testing database